Tracking and positioning using phase information from estimated multi-path components

Zhu, Meifang; Vieira, Joao; Kuang, Yubin; Åström, Karl; Molisch, Andreas; Tufvesson, Fredrik

2015

Tracking and positioning using phase information from estimated multi-path components

Meifang Zhu*, Joao Vieira*, Yubin Kuang†, Kalle Åström†, Andreas F. Molisch ‡, and Fredrik Tufvesson*
*Dept. of Electrical and Information Technology, Lund University, Sweden. Email: *firstname.lastname*@eit.lth.se
†Dept. of Mathematics, Lund University, Sweden. Email: {yubin, kalle}@maths.lth.se
‡Ming Hsieh Dept. of Electrical Engineering University of Southern California, USA. Email: molisch@usc.edu

(Invited Paper)

***Abstract*—High resolution radio based positioning and tracking is a key enabler for new or improved cellular services. In this work, we are aiming to track user movements with accuracy down to centimeters using standard cellular bandwidths of 20-40 MHz. The goal is achieved by using phase information from the multi-path components (MPCs) of the radio channels. First, an extended Kalman filter (EKF) is used to estimate and track the phase information of the MPCs. Each of the tracked MPCs can be seen as originating from a virtual transmitter at an unknown position. By using a time difference of arrival (TDOA) positioning algorithm based on a structure-of-motion approach and translating the tracked phase information into propagation distances, the user movements can be estimated with a standard deviation of the error of 4.0 cm. The paper should be viewed as a proof-of-principle and it is shown by measurements that phase based positioning can be a promising solution for movement tracking in cellular systems with extraordinary accuracy.**

***Index Terms*—Positioning, phase, channel measurements, multipath component, Extended Kalman Filter, time difference of arrival, parameter estimation, tracking.**

I. Introduction

Positioning is a research area that has attracted a lot of attention during the past decades. There has been a tremendous development of positioning technologies based on Global Navigation Satellite Systems (GNSS), such as the Global Positioning System (GPS) and GLONASS, which provide location information around the globe through a constellation of at least 24 satellites [1]. However, the accuracy of GNSS is usually limited and the GNSS do not work properly in shadowed areas, such as inside buildings and close to tall buildings. Therefore, there has been extensive research in developing new positioning techniques to cover these areas and providing ubiquitous positioning solutions with accuracy down to meters or centimeters, e.g., by radio based positioning.

The use of multi-path components (MPCs) of the radio channel enables new possibilities for precise radio based positioning. In [3] the location of a mobile station is estimated based on time of arrival, angle of arrival and Doppler shift of the MPCs using a LS estimator under a single bounce assumption. In [2] the authors used the time difference of arrival between MPCs and simultaneous localization and mapping to achieve position estimates of the receiver and the scattering points, resulting in an average positioning error around 10 m using radio signal measurements with a bandwidth of 100 MHz. To achieve even better positioning accuracy, ultra wideband (UWB) positioning becomes an attractive candidate due to the characteristics of the UWB signals [4]. The operation with GHz of bandwidth allows distances to be resolved with centimeter accuracy, mainly due to the fine delay resolution. However, bandwidth is an expensive resource and it would be beneficial to use already available radio signals with standard cellular bandwidths for positioning. How to obtain the same accuracy as in UWB systems, but using a smaller bandwidth, is an open issue.

To address the problem, let us take a step back and consider wireless propagation channel characteristics. Wireless channels are often described by a sum of MPCs, which carry information about propagation distances in terms of delay and phase. When the MPCs propagate, the delay and phase are varying at the same time. Delay estimates, which e.g. are used in UWB systems to estimate propagation distances, are usually limited by the bandwidth while the phase is not dependent on the bandwidth, given that the MPCs can be resolved. Generally speaking, a 2π rotation of the phase corresponds to a propagation distance of one wavelength. Usually, cellular systems are operating at high carrier frequencies, typically around one or a few GHz, so the corresponding wavelengths are in units of centimeters. If frequent measurements are conducted during one wavelength movement, so that phase wrap-arounds are avoided, the position accuracy can get down to centimeters or even millimeters consequentially. Therefore, it becomes attractive to utilize phase information for high accuracy positioning within cellular systems.

Phase based positioning and tracking has previously been proposed for Radio Frequency Identification (RFID) systems, where the phase of the dominant LOS component is tracked and used for positioning or tracking purposes, see e.g. [5]. Phase information is also used in a related way to improve the performance of GNSS, through Real Time Kinematics (RTK) and differential phase measurements [6]. In this paper, MPCs of radio channels are treated as originating from virtual, but coherent, transmitters located at unknown positions. An Extended Kalman Filter (EKF) is implemented to estimate and track the phases of each MPCs. The relative propagation distance of each MPC is then estimated from the tracked phase information. Relative movements are finally estimated with a structure-of-motion approach that previously has been successfully applied to UWB measurements for movement tracking [11]. To the authors' best knowledge, such a phase based approach for tracking and positioning purpose has not been proposed or demonstrated before.

The paper is structured as follows. Phase estimation and tracking, including the implementation of the EKF algorithm, are discussed in Section II. Section III gives details of an indoor measurement campaign at 2.6 GHz and tracked phases of the MPCs from the measured channels are analyzed. Section IV discusses the used positioning algorithm and presents the tracked movements. Finally, conclusions in Section V wrap up this paper.

II. Phase Estimation and Tracking

Phase is a sensitive propagation parameter and it is affected by the propagation medium, as well as the structure and shape of interacting objects. It is a challenging task to estimate and track such propagation parameters. In traditional approaches, parameters describing specular propagation paths are estimated in a per-snapshot fashion, since channel snapshots are assumed independent and identically distributed, as in SAGE [7]. From these independent estimates, a tracking algorithm can be applied to obtain the time variant performances [8]. Recently, there are a few methods based on state-space modeling for estimation and tracking of propagation parameters simultaneously, including extended Kalman filter (EKF) [9] and particle filter [10] algorithms. In [10], it is shown that the computational complexity of the particle filter algorithm is increasing significantly as the number of estimated and tracked paths is growing. Therefore, EKF is chosen as our solution for parameter estimation and tracking. In the following subsections, the dynamic model and the EKF implementation are discussed for estimation and tracking of the phases of MPCs.

A. Dynamic Model

To extract the parameters of the MPCs, e.g., delay, angle-of-arrival (AOA), angle-of-departure (AOD) and phase, from the measurements, a double-directional channel model is employed, and thus the radio channel can be represented as:

$$\mathbf{H}(f) = \sum_{l=1}^{\mathrm{L}} \gamma_l \mathrm{e}^{-j2\pi f \frac{d_l}{c}} \mathbf{G}_{\mathrm{Rx}}(\varphi_{\mathrm{Rx},l}, \theta_{\mathrm{Rx},l}) \mathbf{G}_{\mathrm{Tx}}(\varphi_{\mathrm{Tx},l}, \theta_{\mathrm{Tx},l})^{\mathrm{T}}, \quad (1)$$

where $\mathbf{G}_{\mathrm{Rx}}$ and $\mathbf{G}_{\mathrm{Tx}}$ are the antenna responses at AOA $(\varphi_{\mathrm{Rx},l}, \theta_{\mathrm{Rx},l})$ and AOD $(\varphi_{\mathrm{Tx},l}, \theta_{\mathrm{Tx},l})$ of the lth path, d_l is the propagation distance of the lth path, L is the number of MPCs and c is the speed of light. Further, γ_l is a complex gain coefficient that is assumed to be slowly varying with respect to both distance and frequency and takes into account distance dependent path loss as well as the phase and amplitude responses of scattering, diffraction and reflection processes. Note, however, that the system model is reformulated in this work as in [9]

$$\mathbf{H}(f) = \sum_{l=1}^{\mathrm{L}} \mathrm{e}^{\alpha_l + j\phi_l} \mathrm{e}^{-j2\pi f \tau_l} \mathbf{G}_{\mathrm{Rx}}(\varphi_{\mathrm{Rx},l}, \theta_{\mathrm{Rx},l}) \mathbf{G}_{\mathrm{Tx}}(\varphi_{\mathrm{Tx},l}, \theta_{\mathrm{Tx},l})^{\mathrm{T}}, \quad (2)$$

where ϕ_l *and* τ_l affect the phase of MPC l and both are estimated independently with the EKF. However, only the phase ϕ_l, called the phase of the MPC, is used for the movement tracking. Note also that α_l represents the logarithm of the amplitude of the l-th MPC.

The parameters of the propagation paths are so represented as

$$\boldsymbol{\mu} = [\ \boldsymbol{\tau}^{\mathrm{T}} \quad \boldsymbol{\varphi}_{\mathrm{Tx}}^{\mathrm{T}} \quad \boldsymbol{\theta}_{\mathrm{Tx}}^{\mathrm{T}} \quad \boldsymbol{\varphi}_{\mathrm{Rx}}^{\mathrm{T}} \quad \boldsymbol{\theta}_{\mathrm{Rx}}^{\mathrm{T}}\ ]^{\mathrm{T}}, \quad (3)$$

$$\boldsymbol{\alpha} = [\ \boldsymbol{\alpha}_{\mathrm{HH}}^{\mathrm{T}} \quad \boldsymbol{\alpha}_{\mathrm{HV}}^{\mathrm{T}} \quad \boldsymbol{\alpha}_{\mathrm{VV}}^{\mathrm{T}} \quad \boldsymbol{\alpha}_{\mathrm{VH}}^{\mathrm{T}}\ ]^{\mathrm{T}}, \quad (4)$$

and

$$\boldsymbol{\phi} = \left[\ \boldsymbol{\phi}_{\mathrm{HH}}^{\mathrm{T}} \quad \boldsymbol{\phi}_{\mathrm{HV}}^{\mathrm{T}} \quad \boldsymbol{\phi}_{\mathrm{VV}}^{\mathrm{T}} \quad \boldsymbol{\phi}_{\mathrm{VH}}^{\mathrm{T}}\ \right]^{\mathrm{T}}, \quad (5)$$

where $\boldsymbol{\tau}$, $\boldsymbol{\alpha}$ and $\boldsymbol{\phi}$ are the vectors containing the delay, the logarithm of the amplitude, and the phase of the MPCs, respectively. The complete polarizations are also considered, e.g., $\boldsymbol{\alpha}_{\mathrm{VH}}$ and $\boldsymbol{\phi}_{\mathrm{VH}}$ represent the logarithmic amplitude and phase, respectively, for the vertical-to-horizontal polarization.

Note that, here only the specular propagation paths are considered, but not the diffuse multi-path components (DMCs), which act as interference for positioning purposes and are treated as noise in this work. So the channel observation $\mathbf{h}$ at time k can be approximated as a superposition of specular paths and noise, here approximated as being white and Gaussian:

$$\mathbf{h}_k = \mathbf{s}(\boldsymbol{\mu}_k, \boldsymbol{\alpha}_k, \boldsymbol{\phi}_k) + \mathbf{w}_k, \quad (6)$$

where $\mathbf{s}$ is a nonlinear equation originating from the channel model in (2) and $\mathbf{w}$ is white Gaussian noise.

To form a dynamic model of the propagation parameters, it is assumed that the propagation parameters are correlated over subsequent measurement snapshots and, specifically, depending linearly on the distance traveled. There have been a number of linear dynamic models for tracking purposes. In this work, a constant velocity model is employed, and it has also previously been shown that this model can give proper tracking performance of propagation parameters [9]. The state vector of the parameters $\mathbf{x}$ at time k is given as

$$\mathbf{x}_k = \left[\ \boldsymbol{\mu}^{\mathrm{T}} \quad \Delta\bar{\boldsymbol{\mu}}^{\mathrm{T}} \quad \boldsymbol{\alpha}^{\mathrm{T}} \quad \boldsymbol{\phi}^{\mathrm{T}} \quad \Delta\bar{\boldsymbol{\phi}}^{\mathrm{T}}\ \right]^{\mathrm{T}}, \quad (7)$$

where $\Delta\bar{\boldsymbol{\mu}}$ and $\Delta\bar{\boldsymbol{\phi}}$ are the vectors with corresponding velocities for their belonging parameters. The discrete-time state transition equation is then defined as:

$$\mathbf{x}_k = \mathbf{F}\mathbf{x}_{k-1} + \mathbf{v}_k, \quad (8)$$

where $\mathbf{F}$ is the state transition matrix. For a single path, $\mathbf{F}$ is composed as

$$\mathbf{F}_{|L=1} = \begin{bmatrix} \mathbf{I}_5 & \mathbf{I}_5 & \mathbf{0} & \mathbf{0} & \mathbf{0} \\ \mathbf{0} & \mathbf{I}_5 & \mathbf{0} & \mathbf{0} & \mathbf{0} \\ \mathbf{0} & \mathbf{0} & \mathbf{I}_4 & \mathbf{0} & \mathbf{0} \\ \mathbf{0} & \mathbf{0} & \mathbf{0} & \mathbf{I}_4 & \mathbf{1}_4 \\ \mathbf{0} & \mathbf{0} & \mathbf{0} & \mathbf{0} & \mathbf{I}_4 \end{bmatrix}, \tag{9}$$

and $\mathbf{v}_k$ is the state noise following a Gaussian distribution with covariance matrix $\mathbf{Q}$.

This model is optimized to track MPCs resulting from smooth movements. However, there can be non-smoothness in some specific scenarios, e.g., at the corners of a square movement. In such situations, this model can show a performance degradation and also diverge in some cases. To cope with this, state noise with large variance is needed, such that the model allows more random deviations.

B. Extented Kalman Filter Design

An extended Kalman filter is implemented for the purpose of estimation and tracking of the phases of the MPCs. The EKF structure is reviewed here for convenience, but the interested reader is referred to [9] for further details. The EKF algorithm consists of two steps, namely prediction and correction:

Prediction:

$$\hat{\mathbf{x}}_{(k|k-1)} = \mathbf{F}\hat{\mathbf{x}}_{(k-1|k-1)} \tag{10}$$

$$\mathbf{P}_{(k|k-1)} = \mathbf{F}\mathbf{P}_{(k-1|k-1)}\mathbf{F}^T + \mathbf{Q} \tag{11}$$

Correction:

$$\mathbf{P}_{(k|k)} = \left(\mathbf{P}^{-1}_{(k|k)} + \mathbf{J}(\hat{\mathbf{x}}_{(k|k-1)})\right)^{-1} \tag{12}$$

$$\Delta\hat{\mathbf{x}}_k = \mathbf{P}_{(k|k)}\mathbf{q}(\mathbf{h}_k|\mathbf{x}_{k|k-1}) \tag{13}$$

$$\hat{\mathbf{x}}_{(k|k)} = \hat{\mathbf{x}}_{(k|k-1)} + \Delta\hat{\mathbf{x}}_k. \tag{14}$$

The prediction step gives the predictions based on the previous state and the transition matrix. The filter error covariance $\mathbf{P}_{(k|k)}$ is also estimated in a similar manner considering the influence of the noise. The correction step aims to decrease the errors by using the recently observed sample to correct the prediction. In the correction step, the first and the second order partial derivatives of the log-likelihood function of the measurement model are used. These are defined as

$$\mathbf{q}(\mathbf{h}|\mathbf{x}) = 2 \cdot \Re\{\mathbf{D}(\mathbf{x})^H(\mathbf{h} - \mathbf{s}(\mathbf{x}))\}, \tag{15}$$

and

$$\mathbf{J}(\mathbf{x}) = 2 \cdot \Re\{\mathbf{D}(\mathbf{x})^H\mathbf{D}(\mathbf{x})\}, \tag{16}$$

respectively, where $\mathbf{D}(\mathbf{x})$ is the first-order partial derivatives with respect to the parameters $\mathbf{x}$ of the observation model $\mathbf{s}(\mathbf{x})$.

III. EXPERIMENTAL INVESTIGATION

Experiments are performed for the purpose of positioning with tracked phases of MPCs from measured radio channels. In this section, the measurement campaign is described in detail, followed by phase tracking for a circular and a square movement, where both smooth and rapidly changing movements are experienced.

A. Channel Measurements

The measurements were conducted in a large sports hall, using our RUSK LUND channel sounder. The transfer functions at 161 frequency points of a 40 MHz bandwidth channel were measured at a center frequency of 2.6 GHz. The output power was 27 dBm, and the sounding signal was a periodically repeated multi-tone signal with a length of 3.2 μs. A cylindrical array acts as a base station (BS), and the center of the cylindrical array is about 2.07 m above the ground. The cylindrical array has 128 ports in total, and consists of 4 stacked circles having 16 dual polarized antennas each. A Skycross SMT-2TO6MB-A omni-directional antenna is mounted on a tripod on wheels 1.7 m above the ground to represent a single-antenna user mobile station (MS). The single antenna was moved manually along the predefined movement patterns, see Fig. 1, which are a circle with radius 0.6 m and a square of side length 1 m, until 5000 channel snapshots are harvested. We made sure that the person moving the MS influenced the measurements as little as possible by remaining close to the floor to minimize body reflections, while at the same time not blocking the ground reflection. The measurements were performed in line-of-sight (LOS) conditions and the distances to the centers of the circle and square are 12.6 m and 19.5 m, respectively.

B. Tracked MPCs and Discussions

To have a proper evaluation time, the maximum number of tracked MPCs is set as 30 in the implemented EKF. For positioning purposes, only a limited number of MPCs are needed, so that a subset of the tracked MPCs showing long life times is selected and processed further.

Conventionally, precise delay tracking needs ultra bandwidth or good enough SNR to resolve the MPCs in the delay domain. Fig. 2 shows examples of tracked delays for some of the MPCs from the circular motion measurements. Sinusoidal variations are expected in the delay domain due to the circular motions. However, the tracked delays cannot properly capture this characteristic. Rather they show noisy variations, even sometimes with step-like changes. Note that, estimation and tracking of the phase and delay are performed independently. However, the phase and delay affect each other from a wave propagation point of view, which leads to the inaccuracy in the delay estimates.

The estimated phases are also expected to show sinusoidal shapes for the circular movement. Fig. 3 shows examples of the tracked phase of four MPCs in the vertical-to-vertical polarization, where the sinusoidal patterns are clearly captured. It can be interesting to note the maximum phase difference

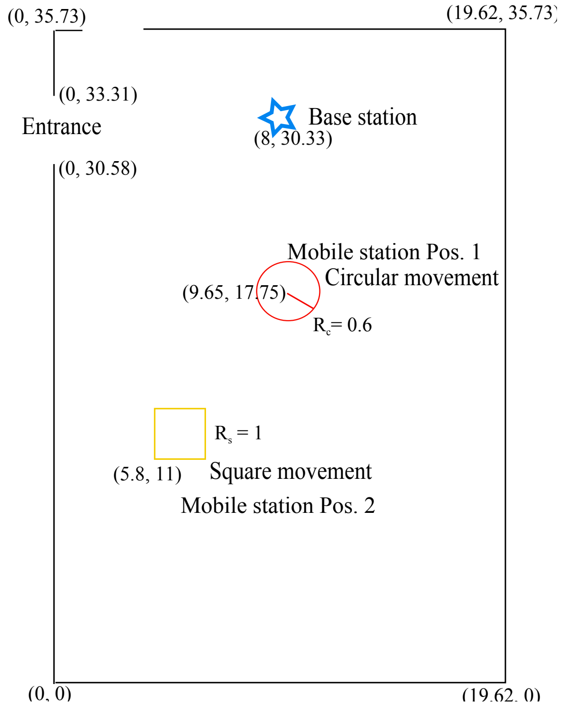

Fig. 1. The geometry of the measurement area and the movement patterns. Coordinates are in meters.

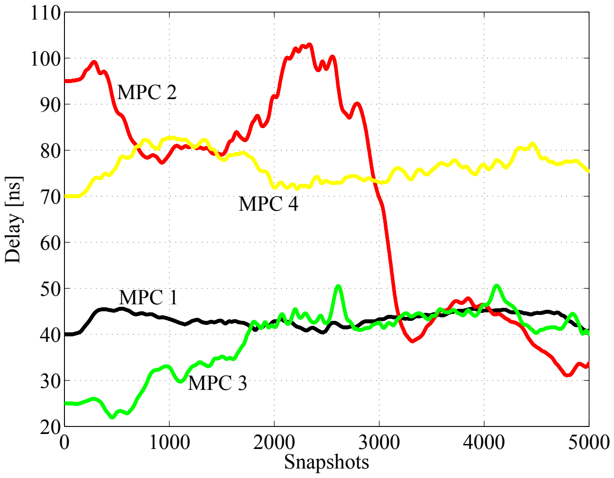

Fig. 2. Tracked delays of a number of MPCs for the circular movement measurements.

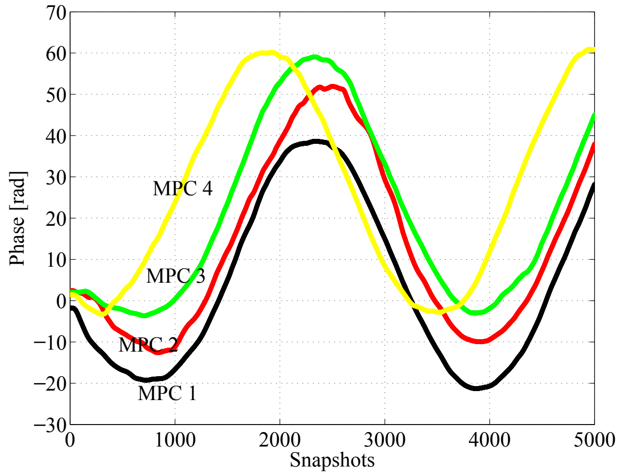

(a) Circular movement

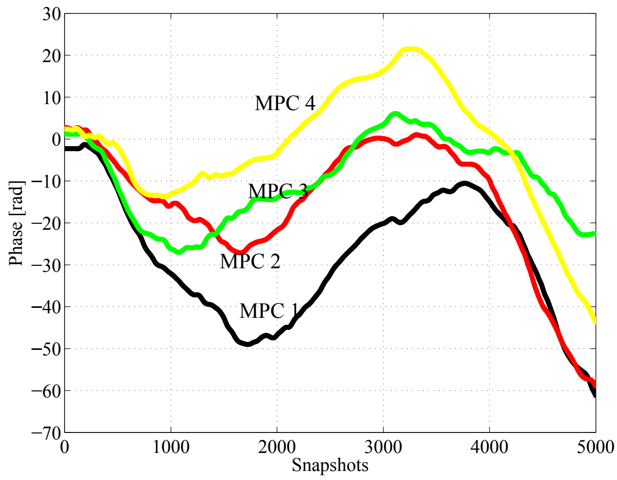

(b) Square movement

Fig. 3. Tracked phases of a number of MPCs for the (a) circular and (b) square movement measurements.

TABLE I
ESTIMATED AZIMUTH AND ELEVATION ANGLE OF THE FOUR MPCS BOTH IN CIRCULAR AND SQUARE MOVEMENTS AT THE BASE STATION SIDE.

MPCs	Circular movement Est.		Square movement Est.	
	Azi. [deg]	Ele. [deg]	Azi. [deg]	Ele. [deg]
MPC 1	282	104	144	64
MPC 2	92	100	348	74
MPC 3	190	102	356	72
MPC 4	160	92	152	46

of each MPC is around 62 radians. Consequently, it reflects the maximum distance change that is approximately 1.2 m, which also corresponds to the diameter of the circle. Note that, some of the MPCs have phase differences slightly less than 62 radians. That is primarily due to that these MPCs stem from scatterers, which are not in the same plane as the single antenna MS. Thus, the scatterers see a slightly projected and scaled copy of the circle, which leads to the projection of the phases of the corresponding MPC.

For the square movement case, we note that at the corners of the square, the movement follows a stop-and-go behavior since it was moved manually. This movement is not considered as smooth. Thus, the tracking tolerance of the filter was increased by defining a higher variance for the process noise to help tracking this sharp change while staying with the same dynamic model. For the square movement, an anti-symmetric pattern in phase is expected. Fig. 3 shows four tracked MPCs from the square movement measurements, where it can be noted the anti-symmetric pattern is observed for each of the MPCs. However, at the corner of the square, the phase does not show a sharp change in slope. Instead, a smooth transition around the corners takes place. This is a consequence of smoothing by the EKF. Also the maximum phase difference of an MPC is around 40 radians, which corresponds to a

TABLE II
STEPS OF THE FAR FIELD TDOA POSITIONING ALGORITHM [11].

Give the measurement matrix D of size 4 x 6.
1) Set $\bar{D}_{i,j} = d_{i,j} - d_{1,j}$
2) Remove the first row of $\bar{D}$
3) Calculate a singular value decomposition $\bar{D} = USV^T$
4) Set $\bar{R}$ to first 3 columns of U and $\bar{N}$ to first 3 columns of SV^T
5) Solve for the six unknowns in the symmetric matrix B using the 6 linear constraints $\bar{n}_j^T B \bar{n}_j = 1$.
6) Calculate A by Cholesky factorization of B, so that $A^T A = B$.
7) Transform motion according to $R = (\bar{R}A^{-1})^T$ and structure according to $N = A\bar{N}$.

movement around 0.75 m. Compared to the predefined 1 m^2 square, the movement is somewhat scaled due to the projection issue.

To have a thorough understanding of the projected phases, the elevation angles at the MS side are needed for each of the MPCs, which cannot easily be obtained due to the single antenna set up. However, it can be noted that the BS and MS are roughly in the same plane. If a single interaction is assumed and the room geometry is known, the elevation angles at the MS side can be estimated roughly. Table I lists the elevation angle at the BS side for the circular and square movements. It can be noted that the differences between the plane of the BS and the planes of the scatterers are approximately 10 degrees at maximum for the circular movement. Thus, the differences between the plane of scatterers and the MS are also insignificant as well as the projections of the tracked phase for the circular movement. For the MPCs of the square movement, a maximum angle difference of 44 degrees is observed between the scatterers and the plane of the BS. With the single interaction assumption, the MS will see the scatterers from the ceiling with an elevated angle, which causes large differences between the plane of scatterers and the plane of MS. Therefore, the propagation distance of each MPC will be scaled and projected.

C. Positioning Results

We are aiming for positioning based on relative movements in this work. Therefore, a TDOA positioning algorithm based on the structure-of-motion problem at hand is utilized and summarized in Table II. A detailed description of the algorithm can be found in [11].

The input to the TDOA positioning algorithm is the measured distance matrix $\bar{\text{D}}$, whose columns are MPCs and rows are estimated relative distances for each channel snapshot. Therefore, the tracked phases are translated into distance to form the matrix $\bar{\text{D}}$. Specifically the distance for the lth MPC at snapshot k is defined as

$$d_{l,k} = c\tau_{\text{ref}} + \frac{(\phi_k - \phi_{\text{ref}})}{2\pi}\lambda \tag{17}$$

where c is the speed of light, τ_{ref} is the selected reference delay, e.g., the estimated delay of the first snapshot, ϕ_{ref} is the selected reference phase, ϕ_k is the phase at snapshot k,

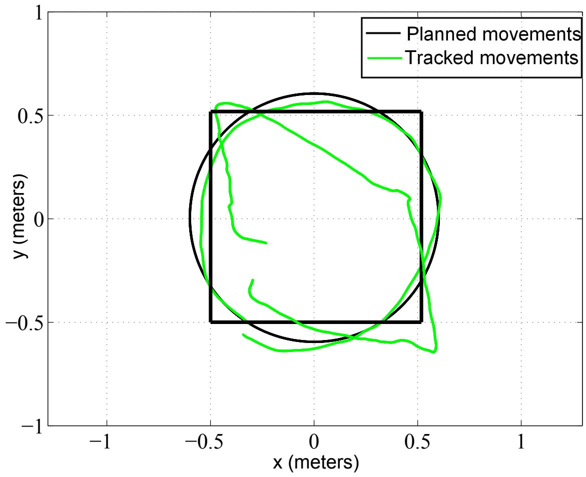

Fig. 4. Positioning results for circular and square movements.

and λ is the wavelength. By singular value decomposition of $\bar{\text{D}}$, the user movement can be estimated.

Fig. 4 shows the estimated movements together with the predefined moving patterns. As stated before, the virtual transmitters and the MS are not in the same plane. Therefore, the movements are slightly projected as well. For the circular movement, it can be noted that the offset between the planned circular movement and the tracked movement is 5 centimeters in maximum, and more than 50% of the locations are within 2 centimeter offset. The overall standard deviation of the circular movement is estimated as

$$\sigma = \sqrt{\frac{1}{n}\sum_{i=1}^{n} |r_{\text{true},i} - r_{\text{est},i}|^2}. \tag{18}$$

where $r_{\text{true},i}$ is the true position (planned route), $r_{\text{est},i}$ is the estimated position and $n = 3120$. The standard deviation of the errors is approximately 4.0 cm. For the square movement, such comparison is not conducted due to the projection issue. Nonetheless, still it can be seen that the square movement can result in reasonably well projected movement estimate. If we assume the propagation environment is known, e.g. through floor plan information, we can actually compensate for the projection error as long as we are dealing with single reflections or interactions. However, for the proof-of-principle in this paper, this is out of scope of the investigation.

IV. CONCLUSIONS

We have implemented an Extended Kalman Filter to perform phase tracking of MPCs for positioning purposes. With the tracked phase information, the relative distance changes of each MPC are observed. By using the structure-of-motion based TDOA positioning algorithm, relative movements have been estimated with accuracy down to centimeters. Our investigation has shown that with the 40 MHz bandwidth, the phase information of each MPCs can be properly estimated and tracked from the radio channels, which can be consequently translated into estimation of time-of-arrival. Therefore, and as the MPCs are coherent, positioning with accuracy down to centimeters is also possible with a limited bandwidth by using phase information. Overall, phase based positioning is a promising technique for tracking and localization purposes. However, there are still challenges for phase based positioning, such as in harsh environments, the phases are discontinuous. So additional information, such as proper delay estimates are needed to adjust the phase estimates. This is initial work, investigations of different movement patterns, e.g., 3D movements, the influence of DMC, and the initial position estimate will be performed in future work.

V. ACKNOWLEDGEMENT

This work has been funded by grants from the Swedish Science Council, the Foundation for Strategic Research and the strategic research area ELLIIT. The authors would like to thank Ghassan Dahman and Jose Flordelis for their help with the measurements.

REFERENCES

[1] J. J. Spilker, Jr., "GPS signal structure and performance characteristics," *Journal of the Institute of Navigation*, vol. 25, no. 2, pp. 121-146, Summer 1978.

[2] C. Gentner, and T. Jost, "Indoor positioning using time difference of arrival between multipath components," in *Proc. IEEE Int. Conf. on Indoor Positioning and Indoor Navigation (IPIN)*, Montbeliard-Belfort, France, Oct. 2013, pp. 1-10.

[3] R. Ramlall, Jie Chen, and A.L. Swindlehurst, "Non-line-of-sight mobile station positioning algorithm using TOA, AOA, and Doppler-shift", *Ubiquitous Positioning Indoor Navigation and Location Based Service (UPINLBS)*, 2014, pp.180-184, Nov. 2014

[4] S. Gezici et al., "Localization via ultra-wideband radios: a look at positioning aspects for future sensor networks," *IEEE Signal Processing Magazine*, vol. 22, no. 4, pp. 70-84, Jul. 2005.

[5] P. V. Nikitin et al., "Phase based spatial identification of UHF RFID tags," in *Proc. IEEE RFID 2010*, Orlando, FL, Apr. 2010, pp. 102-109.

[6] Real-Time Kinematic surveying training Guide, part number 33142-40, Revision D, Sep. 2003, [Online]. Available: http://gpstraining.com/downloads/MANUALS-QUICK%20GUIDES/RTKTrainingRevD.pdf.

[7] B. H. Fleury, M. Tschudin, R. Heddergott, D. Dahlhaus, and K. Ingeman Pedersen, "Channel parameter estimation in mobile radio environments using the SAGE algorithm," *IEEE J. Select. Areas Commun.,* vol. 17, no. 3, pp. 434-450, Mar. 1999.

[8] N. Czink, R. Tian, S. Wyne, F. Tufvesson, J. P. Nuutinen, J. Ylitalo, E. Bonek and A. F. Molisch, "Tracking time-variant cluster parameters in MIMO channel measurements," in *Proc. China Commun. Conf.*, Shanghai, China, 2007, pp. 1147-1151.

[9] J. Salmi, A. Richter, and V. Koivunen, "Detection and tracking of MIMO propagation path parameters using state-space approach," *IEEE Transactions on Signal Processing*, vol. 57, no. 4, pp. 1538-1550, Apr. 2009.

[10] X. Yin, G. Steinbock, G. Kirkelund, T. Pedersen, P. Blattnig, A. Jaquier, and B. Fleury, Tracking of time-variant radio propagation paths using particle filtering, in *Proc. IEEE Int. Conf. Communications (ICC08)*, May 2008, pp. 920924.

[11] Y. Kuang, K. Åström, and F. Tufvesson, "Single antenna anchor-free UWB positioning based on multipath propagation," in *Proc. IEEE Int. Conf. Communications (ICC'13)*, Budapest, Hungary, Jun. 2013, pp. 5814-5818.